# A Wideband, Simultaneous Amplitude-Phase-Control Unit Cell for Shaped-Beam Transmitarray Antennas

Sen Liu
Radio Research Institute
National Institute of Information and Communications Technology
Tokyo, Japan
liusen@nict.go.jp

Qiang Chen
Department of Communications Engineering
Tohoku University
Sendai, Japan
qiang.chen.a5@tohoku.ac.jp

***Abstract*—In this paper, a transmitarray unit cell with simultaneous amplitude and phase control capability is presented. The unit cell is wideband and provides full-coverage for both amplitude and phase control, demonstrating promising potential for shaped-beam transmitarray antennas.**

***Keywords—amplitude control, shaped beam, transmitarray, unit cell***

## I. Introduction

As alternatives to lens antennas and phased array antennas, transmitarray antennas (TAs) have attracted much attention in recent years, providing distinctive advantages of high efficiency, low profile, lightweight, low-cost, and easy-to-fabricate. Composed of a large number of individual unit cells, TAs are able to generate a forward beam with desired characteristics. As a vital component of TAs, unit cells are highly related to system performances and function realization such as a shaped-beam radiation pattern. This paper presents a transmitarray unit cell with capability of simultaneous amplitude and phase control. The unit cell is wideband and flexible, providing promising potentials for shaped-beam transmitarray antennas.

## II. Design and Analysis of the Unit Cell

The 3-D perspective view of the unit cell, together with the components of the incident (green), reflected (blue), and transmitted (red) fields, is shown in Fig. 1(a). It is composed of three metal layers (yellow parts), which are etched on three dielectric substrates ($\varepsilon_r = 3.3$, $\tan\delta = 0.001$, $T_{sub} = 0.8$ mm) separated by the same air gaps ($T_{air} = 4.0$ mm). The top and bottom layers are two identical orthogonal-positioned grid polarizers with strip width of $s = 0.8$ mm and gap of $w = 2.2$ mm. An obliquely-placed ($\theta$) shaped dipole with radius of $R_1$, dipole width of $w_1$, and dipole length of $L$, is printed on the middle layer, where the detailed top view is presented in Fig. 1(b). Besides, the periodicity of the unit cell is $P = 15$ mm, which is equivalent to $0.5\lambda_0$, where $\lambda_0$ denotes the free-space wavelength at 10 GHz. The element responses are highly dependent on the polarization of the incident fields. Specifically, with y-polarized illumination ($E_i^y$), the combined layers form a Fabry-Pérot-like cavity [1], resulting in the interference between the multiple polarization couplings. By rotating $\theta$, the consequent Cr-Pol transmissive ($E_t^x$) interference can either be constructive or destructive, leading to the manipulation of the $|E_t^x|$. One should be pointed out that the control of the magnitude ($|E_t^x|$) is at the cost of the reduced transmission efficiency. Considering the grid orientation of the top and bottom layers, in order to attenuate $|E_t^x|$, part of the power should be reflected by means of $E_r^y$. As a consequence, the antenna system inevitably suffers from less efficiency. However, the undesired $E_r^y$ component is isolated on the reflection side. Meanwhile, the phase of the $E_t^x$

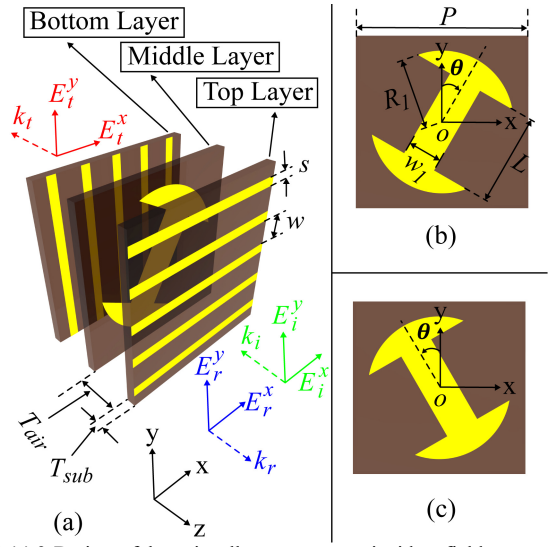


Fig.1 (a) 3-D view of the unit cell; green arrows: incident field components; blue arrows: reflected field components; red arrows: transmitted field components. (b) Top view of the middle layer. (c) Top view of the mirrored middle layer.

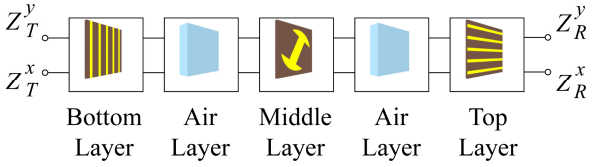


Fig. 2 Equivalent S-parameter network representation of the unit cell.

TABLE I
Final Design Parameters of the Unit Cell

| | |
|---|---|
| $R_1$ | 6.5, 6.8, 7.1 mm |
| $w_1$ | 3.0 mm |
| $L$ | 1.0~12.8 mm ($R_1$=6.5)<br>1.0~13.4 mm ($R_1$=6.8)<br>1.0~14.0 mm ($R_1$=7.1) |
| $\boldsymbol{\theta}$ | 0°~45° |

component can be controlled by varying $L$. On the other hand, the fields are fully reflected in the form of $E_r^x$ with x-polarized incident waves ($E_i^x$), which means the Cr-Pol of the feed source has little effect on the transmission side. Therefore, the antenna system is able to exhibit high polarization purity on the transmission side, especially in beam region.

Generalized-scattering-matrix-based [2] cascaded S-parameter network is introduced to analyze the unit cell, where the schematic of the equivalent network is shown in Fig. 2. Each layer is packed as a building block. The port superscripts denote the x-/y-polarized fields, and the subscripts represent reflection or transmission side. Variables in the network exist only in the middle layer. Therefore, the element response can be obtained very efficiently once that of the single middle layer is known. Meanwhile, due to the presence of the air gap, high-order space harmonics have little effect on the results, leading to high accuracy of the network simulation. The performance of the element can be fully characterized by two matrix equations shown in the following:

$$\begin{pmatrix} E_t^x \\ E_t^y \end{pmatrix} = \overline{\overline{\boldsymbol{T}}} \bullet \begin{pmatrix} E_i^x \\ E_i^y \end{pmatrix} \tag{1}$$

$$\begin{pmatrix} E_r^x \\ E_r^y \end{pmatrix} = \overline{\overline{\boldsymbol{R}}} \bullet \begin{pmatrix} E_i^x \\ E_i^y \end{pmatrix} \tag{2}$$

$$\overline{\overline{\boldsymbol{T}}} = \begin{bmatrix} T_{xx} & T_{xy} \\ T_{yx} & T_{yy} \end{bmatrix} \tag{3}$$

$$\overline{\overline{\boldsymbol{R}}} = \begin{bmatrix} R_{xx} & R_{xy} \\ R_{yx} & R_{yy} \end{bmatrix} \tag{4}$$

where $E_{i/r/t}^{x/y}$ represents the incident/reflected/transmitted field for the unit cell with x or y polarization. The complex matrices $\overline{\overline{\boldsymbol{R}}}$ and $\overline{\overline{\boldsymbol{T}}}$ describe the transmission and reflection performance of the unit cell. Here, the first letter of the subscript denotes the polarization of reflected or transmitted fields, along with the second letter for that of incident fields. In this design, $T_{xy}$ is of interest. After huge parametric studies and geometric optimization, the final design parameters are listed in Table I. Three discrete values of $R_1$ are selected to fulfill the requirements.

The $T_{xy}$ responses evaluated in different configurations are plotted in polar diagram shown in Fig. 3. Full amplitude coverage and half phase coverage can be achieved directly. The other half space can be easily obtained by mirroring the middle layer, where the top view is shown in Fig. 1(c), consequently leading to full coverage of both amplitude and phase responses. The frequency responses in element configuration of $R_1 = 6.8$ mm are given in Fig. 4(a) and (b). Smooth amplitude responses and linear phase responses can be obtained, illustrating the potentials of wideband operation.

## III. Conclusion

In this paper, a novel transmitarray unit cell with simultaneous amplitude and phase control capability has been proposed. The unit cell was studied and analyzed. Amplitude and phase control with both full-coverage were obtained by varying three geometric parameters. The unit cell can be used for shaped-beam transmitarray antennas.

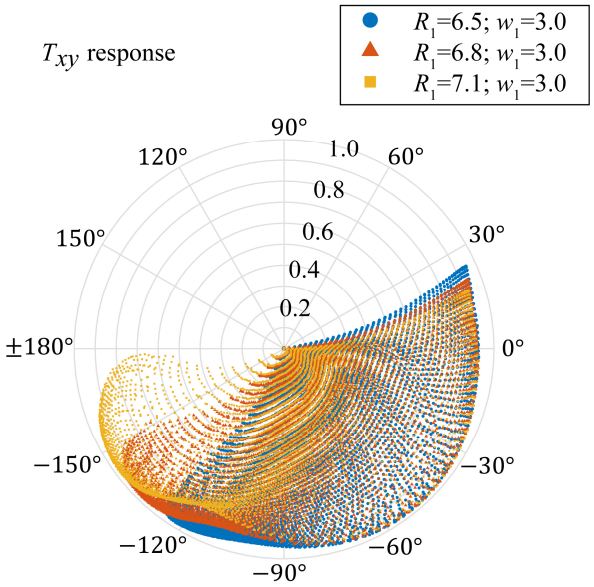


Fig. 3 Polar diagram of $T_{xy}$ response. All the results are evaluated at 10 GHz.

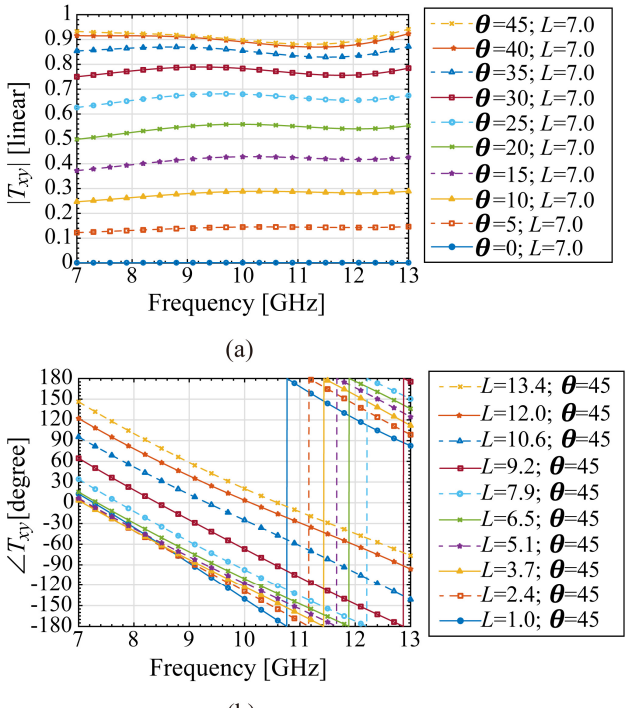


Fig. 4 (a) Frequency response of $|T_{xy}|$ with fixed value of $L$ and discrete values of $\theta$. (b) Frequency response of $\angle T_{xy}$ with fixed value of $\theta$ and discrete values of $L$. All the results are based on the unit cell configuration of $R_1 = 6.8$ mm.

## References

[1] H.-T. Chen, J. Zhou, J. F. O'Hara *et al.*, "Antireflection Coating Using Metamaterials and Identification of Its Mechanism," *Phys. Rev. Lett.*, vol. 105, no. 7, pp. 073901, Aug. 2010.

[2] R. Mittra, C. H. Chan, and T. Cwik, "Techniques for analyzing frequency selective surfaces-a review," *Proc. IEEE*, vol. 76, no. 12, pp. 1593-1615, 1988.